Biosensors and Bioelectronics 31 (2012) 182–189

Contents lists available at SciVerse ScienceDirect

Biosensors and Bioelectronics

journal homepage: www.elsevier.com/locate/bios

Ultrasensitive indicator-free and enhanced self-signal nanohybrid DNA sensing platform based on electrochemically grown poly-xanthurenic acid/Fe_2O_3 membranes

Wei Zhang[a,b,1], Tao Yang[a,1], Kui Jiao[a,*]

[a] State Key Laboratory Base of Eco-chemical Engineering, College of Chemistry and Molecular Engineering, Qingdao University of Science and Technology, Qingdao 266042, China
[b] School of Chemistry and Chemical Engineering, Linyi University, Linyi 276005, China

ARTICLE INFO

Article history:
Received 29 July 2011
Received in revised form
30 September 2011
Accepted 11 October 2011
Available online 18 October 2011

Keywords:
Poly-xanthurenic acid
Fe_2O_3 substrate
Self-signal
Indicator-free impedance
PML/RARA fusion gene

ABSTRACT

This paper describes a novel electrochemical DNA biosensor for simple, rapid, and specific detection of PML/RARA fusion gene in acute promyelocytic leukemia by using 18-mer single-stranded deoxyribonucleic acid as the capture probe. Nanosized Fe_2O_3 was first immobilized on the surface of a carbon paste electrode (CPE). Then poly-xanthurenic acid (PXa), a new electroactive material, was electrogenerated by using the pulse potentiostatic method on the Fe_2O_3 substrate to form a unique and uniform nanorhombus structure. Due to the unique binding ability of xanthurenic acid (Xa) with Fe_2O_3, Xa monomers tended to be adsorbed around nanosized Fe_2O_3, and the electropolymerization efficiency was greatly improved. Owing to the presence of abundant carboxyl groups, the capture probe was covalently attached on the carboxyl-terminated PXa/Fe_2O_3 nanorhombus membranes through the free amines of DNA sequences based on the 1-ethyl-3-(3-dimethylaminopropyl) carbodiimide and N-hydrosulfosuccinimide cross-linking reaction. The covalently immobilized capture probe could selectively hybridize with its target DNA to form double-stranded DNA on the PXa/Fe_2O_3/CPE surface. Electrochemical impedance spectroscopy was adopted for indicator-free monitoring of the hybridization reaction on the probe-captured electrode. As a result, the efficient probe immobilization platform, coupled with the ultrasensitive indicator-free impedance measurement, gave rise to a detection limit of 2.8 fmol/L and a dynamic range spanning 8 orders of magnitude. The excellent analytical properties of the proposed biosensor developed here holds great promise for ultrasensitive detection of other biorecognition events and diagnosis of diseases in practice.

1. Introduction

The rapid, selective, and sensitive detection of nucleic acid sequences has been extensively applied in life sciences research, clinical diagnosis, environmental and food safety monitoring, gene therapy, pathology, and forensic sciences (Sassolas et al., 2008). A variety of optical, acoustic, gravimetric, and electronic approaches have been employed for the detection of DNA in the past few years (Sharon et al., 2010; Prusty and Herrmann, 2010). However, there were some limitations in these approaches, such as time-consuming, poor precision and expensiveness. Due to their simplicity, reliability, portability, sensitivity, and selectivity as well as compatibility with microfabrication technology, DNA biosensors based on electrochemical transduction have attracted significant attention and become popular (Zhang et al., 2009b; Dong et al., 2010; Kannan et al., 2011). Some of these electrochemical strategies require a label (nanoparticles, enzymes, metal complexes, magnetic beads, or organic redox markers) attached to the DNA target (Marques et al., 2009; Cash et al., 2009; Shiddiky et al., 2010). However, although the labeling step enhances the sensor sensitivity, it markedly increases the time, complexity, and cost of the measurement. Among different electrochemical methods enabling direct detection of DNA hybridization, electrochemical impedance spectroscopy (EIS) transduction is the goal of numerous research works due to portability and low power requirement and cost. EIS is a powerful technique for the characterization of electrochemical systems and therefore constructs a sensitive and efficient tool for the characterization of biofunctionalized electrodes. This technique is especially interesting for label-free DNA detection since it bypasses the need to modify DNA molecules with labels (Kjallman et al., 2008; Zhang et al., 2009a).

The surface immobilization of the ssDNA probe on the electrode is a key step to fabricate the electrochemical DNA biosensor. Nanomaterials, due to their high surface-to-volume ratios, not only can be used to increase the amount of DNA immobilization, but also can

* Corresponding author. Tel.: +86 532 84022665; fax: +86 532 84023927.
E-mail address: kjiao@qust.edu.cn (K. Jiao).
[1] These two authors contributed equally to this work.

0956-5663/$ – see front matter © 2011 Elsevier B.V. All rights reserved.
doi:10.1016/j.bios.2011.10.015

act as a medium to amplify the electrochemical signal. Therefore, various nanomaterials have been reported to act as the support for probe immobilization, such as Au nanoparticles (Wang et al., 2010; Liu et al., 2010), metal oxide nanoparticles (Solanki et al., 2009; Singh et al., 2011), and nanostructured conducting polymers (Hu et al., 2010; Bo et al., 2011). In particular, DNA detection requires the precise location of the ssDNA probe at a transducer surface without loss of biological activity or lack of accessibility, and with appropriate orientation propitious to duplex formation with the DNA target as well as a minimum distance between the duplex and the electrode surface. However, the stable and reproducible immobilization of DNA molecules on a surface with complete retention of their biological activity remains always a crucial problem. In this context, electrogenerated polymeric materials attract wide attention as interfaces between an electrode and the DNA probe due to their easy control over morphology and thickness and the reproducibility of the polymer formation with precise spatial resolutions (Peng et al., 2009). Moreover, the introduction of appropriated functionalities by the chemical modification of the monomer or the membrane can lead to DNA immobilization following various strategies involving electrostatic adsorption, affinity interactions, or chemical grafting. Among traditional conducting polymers, polypyrrole and polyaniline based materials have been applied in DNA biosensing field (Thompson et al., 2003; Riccardi et al., 2008; Zhou et al., 2009). However, the major drawbacks of these traditional polymers are high toxicity and relatively complicated synthesis, which greatly restrict their application in bioelectrochemistry. Xanthurenic acid (Xa) is a product of the tryptophan-NAD pathway, which is of low toxicity and related to various pathological conditions (Shen and Ji, 2008). To the best of our knowledge, the use of poly-xanthurenic acid (PXa) as the platform for DNA immobilization and electrochemical hybridization detection has not yet been reported.

Fe_2O_3, as an environment-friendly n-type semiconductor oxide and the most thermodynamically stable phase of iron oxide under ambient conditions, is drawing intense interest not only for its unique properties but also for its applications in many fields such as magnetic recording media, lithium-ion batteries, anticorrosive agents, water treatment, and pigments (Cao and Zhu, 2008). In particular, nanosized Fe_2O_3 may act as a promising substrate for biosensing owing to its unusual properties including fine biocompatibility, high conductivity, low toxicity, and easy preparation process (Adekunle et al., 2010; Zhang et al., 2010). It should be noted that Xa can act as a potent iron chelator and the hydroxyl group in the 8-position of the quinoline moiety is essential for the binding of iron (Silva et al., 2010), and therefore the presence of nanosized Fe_2O_3 has a distinct influence on the formation of PXa.

Acute promyelocytic leukemia (APL) is a kind of acute leukemia, which often goes with bleeding severely. The bleeding mechanism of the APL patients is very complex. Almost all of the APL patients are characterized by chromosome reciprocal translocation, resulting in the generation of fusion gene between promyelocytic leukemia (PML) and retinoic acid receptor alpha (RARA), which forms PML/RARA fusion gene (Wei et al., 2009). Here, we report, for the first time, an innovative design of an ultrahigh performance indicator-free impedimetric biosensor for the detection of PML/RARA fusion gene based on electropolymerized PXa membrane on nanosized Fe_2O_3 substrate. The formed PXa/Fe_2O_3 nanorhombus membranes combined the fine conductivity and large surface area of Fe_2O_3 and the high density of carboxyl groups of PXa, and could conveniently bind the free amines of DNA probes to carboxyl groups of PXa by using the 1-ethyl-3-(3-dimethylaminopropyl) carbodiimide (EDC) and N-hydrosulfosuccinimide (NHS) cross-linking reaction. The morphologies and electrochemical behaviors of the PXa/Fe_2O_3 nanocomposite membranes were characterized by scanning electron microscopy (SEM) and cyclic voltammetery (CV), respectively. The conformational and concomitant conductivity changes of the DNA/PXa/Fe_2O_3 membranes induced a significant change of self-redox properties of the PXa layer, and CV and EIS were used to investigate the mechanism of the indicator-free direct electrochemical detection of DNA hybridization.

2. Materials and methods

2.1. Apparatus and materials

All the electrochemical measurements were performed on a CHI 660B electrochemical workstation (Shanghai CH Instrument Company, China). A conventional three-electrode system was used with carbon paste electrode (CPE) or the modified CPE as the working electrode, a saturated calomel electrode (SCE) as the reference electrode and a Pt wire as the counter electrode. SEM was carried out using a JSM-6700F machine (JEOL, Tokyo, Japan). FT-IR spectrum was conducted on a Tensor 27 FT-IR spectrophotometer (Bruker Company, Germany).

The synthesis of nanosized Fe_2O_3 and DNA sequences used in experiments can be seen in Supplementary material. 4,8-Dihydroxyquinoline-2-carboxylic acid (xanthurenic acid, Xa) was acquired from Acros Organics (Belgium). EDC and NHS were purchased from Sigma (St. Louis, MO, USA).

2.2. Electrochemical fabrication of PXa/Fe_2O_3 membranes

The fabrication of CPE was carried out by using a method of Jiang (Jiang et al., 2008). Prior to modification, the surface of the electrode was smoothed with a weighting paper. 10 μL of 2.0 mg/mL Fe_2O_3 suspension was spread uniformly onto the fresh surface of CPE and air-dried naturally to obtain the Fe_2O_3/CPE. Then it was immersed in a solution of 400 μmol/L Xa in 0.3 mol/L PBS (pH 5.5) for electropolymerization by pulse potentiostatic method (PPM). The optimal electropolymerization parameters were listed as follows: upper limit potential E_a, 0.6 V; lower limit potential E_c, −0.2 V; and anodic pulse duration T_a, 0.7 s; cathodic pulse duration T_c, 0.3 s; and total pulse time T_{exp}, 2000 s. Prior to all the electropolymerization experiments, the PBS was bubbled with nitrogen for 10 min.

For comparison, CV, potentiostatic deposition (PD) and galvanostatic deposition (GD) were also employed for the electropolymerization of PXa, and their optimal polymerization parameters were listed below: CV, potential span, 1.2 to −0.6 V; scan rate, 50 mV/s; polymerization cycle, 30 cycles; PD, potential, 0.5 V; deposition time, 800 s; GD, current density, 0.01 mA/cm^2; deposition time, 1800 s.

2.3. Immobilization and hybridization of DNA on the PXa/Fe_2O_3 membranes

The ssDNA probes were covalently attached on the PXa/Fe_2O_3/CPE surface through the free amines of DNA probes by using the EDC/NHS cross-linking reaction. The terminal carboxyl groups of the PXa/Fe_2O_3 nanorhombus membranes were activated by immersion in 0.3 mol/L PBS buffer solution (pH 7.0) containing 2.0 mmol/L EDC and 5.0 mmol/L NHS for 1 h. The linker/PXa/Fe_2O_3/CPE was rinsed with 0.3 mol/L PBS (pH 7.0) to wash off the redundant EDC and NHS. 10 μL of Tris–HCl buffer solution (pH 7.0) containing 1.0×10^{-7} mol/L ssDNA probes was then pipetted onto the chemically modified electrode and air-dried to dryness. The electrode surface was washed with 0.5% sodium dodecylsulfate (SDS) solution to remove the unbound DNA probes.

Further, the hybridization reaction was carried out by transferring 10 μL of hybridization solution (2× SSC buffer, pH 7.5)

containing cDNA onto the probe-modified electrode, followed by thoroughly washing the electrode with 0.5% SDS solution to remove the unhybridized DNA. The same procedure as mentioned above was applied to the probe-modified electrode for hybridization with single-base mismatched and ncDNA sequences.

The schematic representation of the immobilization and hybridization of DNA on the PXa/Fe_2O_3 membranes was illustrated in Scheme 1A.

2.4. Electrochemical measurements

The CV measurements were performed with 0.3 mol/L PBS solution (pH 7.0) or 1.0 mmol/L $K_3Fe(CN)_6$ and 1.0 mmol/L $K_4Fe(CN)_6$ solution containing 0.1 mol/L KCl. The CV scan rate was 100 mV/s.

The EIS measurements were carried out under open-circuit conditions, and the supporting electrolyte was 0.3 mol/L PBS solution (pH 7.0). The AC voltage amplitude was 5 mV and the voltage frequencies ranged from 10^5 Hz to 1 Hz.

3. Results and discussion

3.1. Electrochemical synthesis of the PXa/Fe_2O_3 membranes

The conventional electropolymerization methods for the fabrication of conducting polymer membranes were focused on CV, PD and GD. However, the membranes prepared by these methods are always thick and compact, and the compact membranes have relatively small specific surface and poor electrical conductivity, which are unfavorable for the construction of electrochemical biosensors. Compared with traditional electrochemical methods, composite membranes prepared by PPM have larger specific area, higher conductivity, and better electrochemical reaction ability, and can be used as an excellent supporting material for chemical biosensors. Here, the electrochemical properties of the PXa/Fe_2O_3 composite membranes prepared by PPM (Fig. 1A), CV (Fig. 1B), PD (Fig. 1C) and GD (Fig. 1D) were compared by monitoring the self-redox reactions of PXa in 0.3 mol/L PBS (pH 7.0) and curve a was the CV signals at the PXa/CPE, and curve b was the CV signals at the PXa/Fe_2O_3/CPE. As can be observed from Fig. 1A, curve b, the voltammetric response of the PXa/Fe_2O_3/CPE prepared by PPM consisted of a well-shaped quasi-reversible pair of peaks. This could be ascribed to the self-redox reactions of PXa that occur at the electrode surface and the redox process going from quinone structure to hydroquinone structure (Scheme 1B) (Haccoun et al., 2004). In summary, the PXa/Fe_2O_3 membranes prepared by PPM displayed the largest current response, demonstrating that the PXa/Fe_2O_3 membranes prepared by PPM possessed excellent electrical conductivity, which was beneficial for the electron transfer.

As can be seen, the self-redox signals of PXa layer at the composite membranes prepared with Fe_2O_3 by the four electropolymerization methods were all larger than that at the membranes prepared without Fe_2O_3, indicating that the presence of nanosized Fe_2O_3 with large surface area and excellent conductivity was favorable for the electropolymerization of PXa. When the Fe_2O_3 modified electrode was immersed into the Xa solution, as a result of that the hydroxyl group in the 8-position of the quinoline moiety of Xa had the affinity with iron (Silva et al., 2010), considerably high local concentration of Xa monomers could be adsorbed on the surface of nanosized Fe_2O_3. Therefore, the electropolymerization efficiency was greatly improved. The resulting PXa layer with a large surface area could provide more activation sites and consequently enhance the immobilization amount of probe ssDNA.

3.2. SEM characterization

The morphologies of the membranes prepared by different electropolymerization methods were characterized by SEM, as shown in Fig. 2. As can be seen, compared with the PXa membranes prepared by CV (Fig. 2B), PD (Fig. 2C) and GD (Fig. 2D) on the Fe_2O_3 substrate, the PXa membranes prepared by PPM (Fig. 2A) on the Fe_2O_3 substrate revealed a rhombus-like morphology of the nanostructures. The morphologies of the PXa membranes prepared by PPM with and without Fe_2O_3 were also compared. As displayed in Fig. 2E, the PXa prepared by PPM without Fe_2O_3 formed a compact and thick structure, and the compact structure made the membranes have small specific surface area, which did not benefit the electron transfer. In conclusion, the PXa layer prepared by PPM (Fig. 2A) on the Fe_2O_3 substrate displayed rhombus-like nanostructures, which was beneficial for the electron transfer along and among the polymer chains. This might be ascribed to the presence of nanosized Fe_2O_3 with large surface area in the process of electropolymerization of Xa. When the Fe_2O_3/CPE was immersed into the Xa solution, Xa monomers could be adsorbed on the surface of the nanosized Fe_2O_3 through affinity interaction, which resulted in a considerably higher local concentration of Xa around Fe_2O_3. With the application of pulse potentials, Xa around the Fe_2O_3 was first oxidized to free radicals, and then the polymerization reaction was initiated. Therefore, the polymerization efficiency was greatly improved. The resulting PXa layer with a large surface area could provide more activation sites for probe ssDNA immobilization, and further promote the sensitivity of DNA detection.

3.3. FT-IR spectrum characterization

FT-IR spectroscopy is a sensitive method to probe into the structure of biomolecules. A further FT-IR spectrum was recorded to study the chemical immobilization of ssDNA with the polymer as shown in Fig. S1 (see Supplementary material). The infrared absorption peak at 1633 cm^{-1} may be related to the C=O stretching vibration of the amide bonds. The absorption peak at 1584 cm^{-1} may be caused by the combination of N–H bending and C–N stretching vibration of the amide bonds. Therefore, the FT-IR spectrum results for the ssDNA/PXa/Fe_2O_3/CPE revealed that the DNA probes were linked onto the PXa/Fe_2O_3 membranes by forming amide bonds between the carboxyl groups of PXa and amine groups at the ends of ssDNA during EDC/NHS coupling.

3.4. Electrochemical characterization of the PXa/Fe_2O_3 nanorhombi prepared by PPM

CV can provide useful information on the barrier changes of the electrode surface during the fabrication process. Therefore, the CV of 1.0 mmol/L $[Fe(CN)_6]^{3-/4-}$ was chosen as a marker to investigate the changes of the electrode behavior before and after each assembly step, as shown in Fig. 3A. The curve a was the CV of $[Fe(CN)_6]^{3-/4-}$ at the bare CPE, which had no obvious redox peaks. This might be ascribed to the poor electrical conductivity of the bare CPE. After the bare CPE was coated with nanosized Fe_2O_3, as illustrated in curve b, the current response increased obviously ascribed to the good electron-transfer ability and large electroactive surface area of Fe_2O_3. A couple of well-defined redox peaks could be observed at the PXa/CPE (curve c) prepared by PPM. The information of the PXa/Fe_2O_3/CPE was shown in curve d, which had the largest redox peaks. These results indicated that the PXa/Fe_2O_3 nanorhombus membranes with the synergistic amplification effect of Fe_2O_3 and PXa had a much larger effective surface area and better electrical conductivity, which could facilitate the electron transfer of $[Fe(CN)_6]^{3-/4-}$.

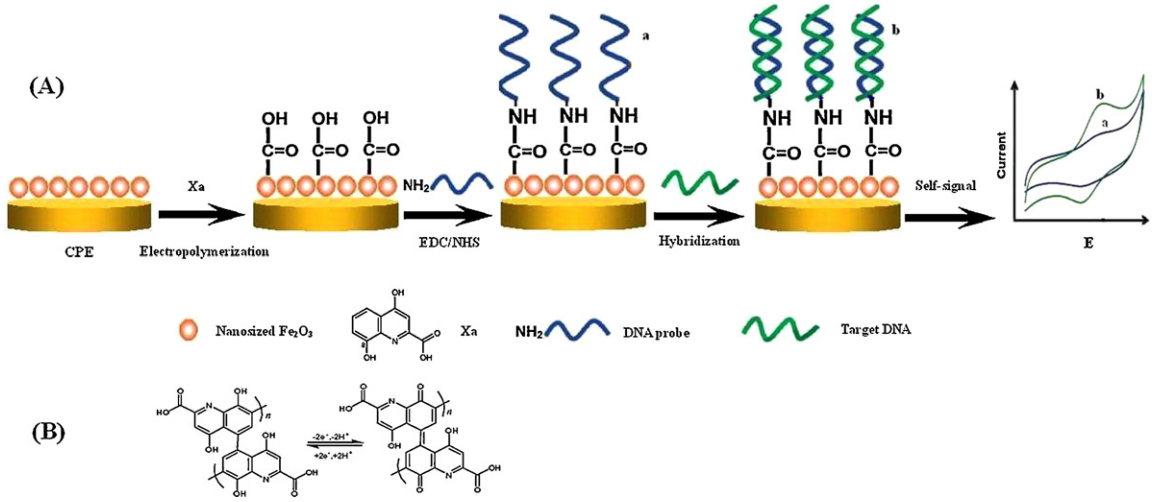

Scheme 1. (A) Schematic representation of the immobilization and hybridization of DNA on the PXa/Fe_2O_3 membranes. (B) The self-redox process of PXa layer at the electrode surface.

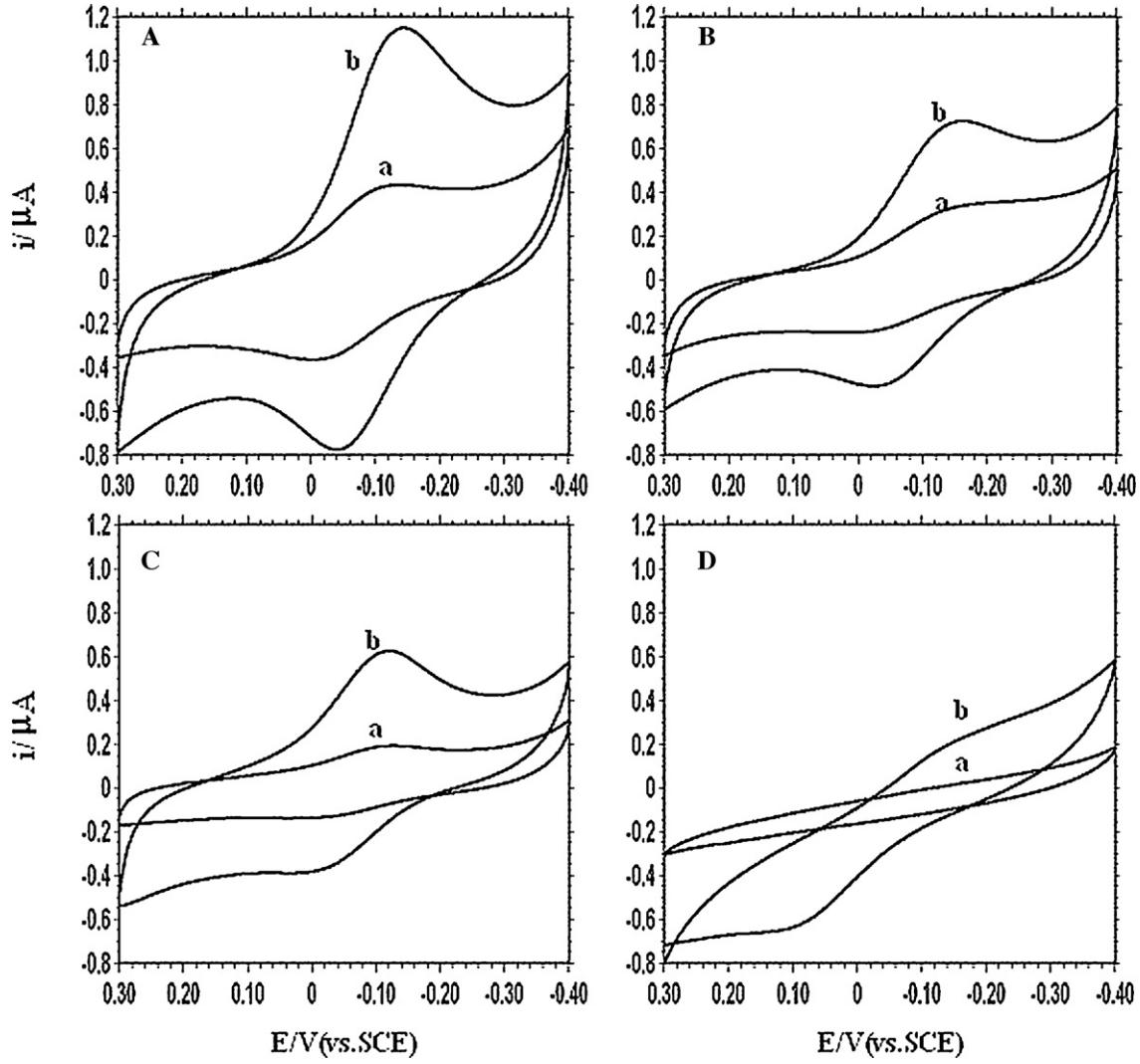

Fig. 1. CVs of the PXa/CPE (a) and PXa/Fe_2O_3/CPE (b) prepared by (A) PPM, (B) CV, (C) PD and (D) GD recorded in 0.3 mol/L PBS (pH 7.0). Scan rate: 100 mV/s.

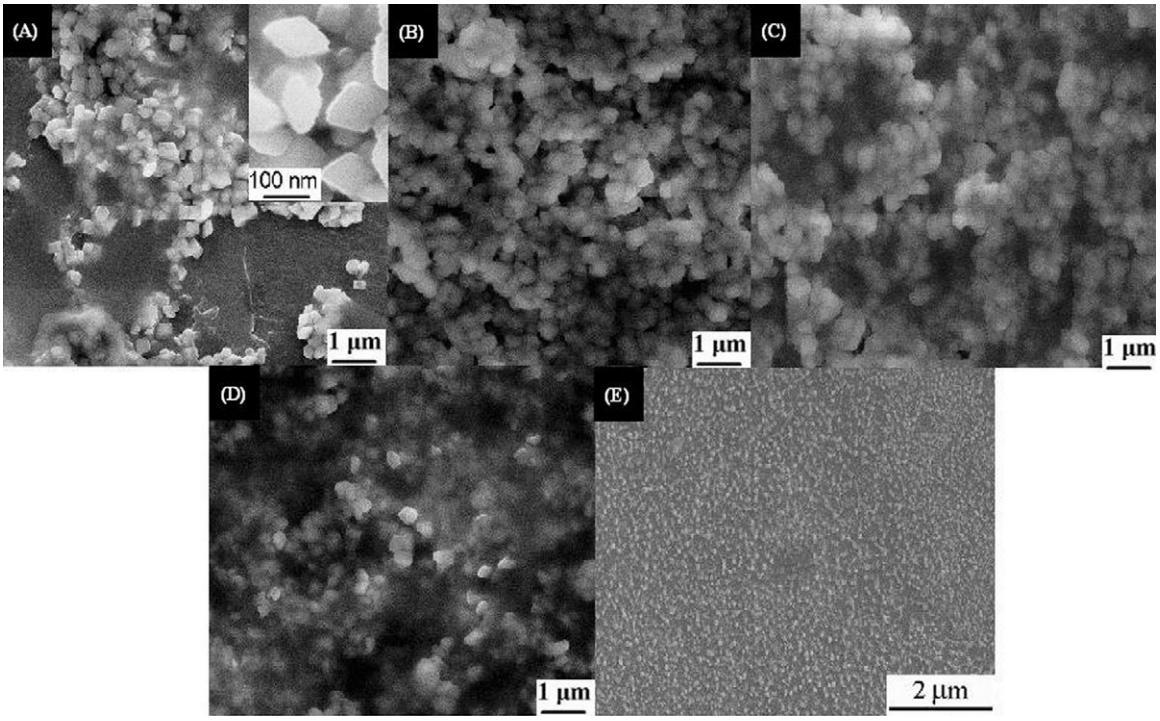

Fig. 2. SEM images of the PXa/Fe_2O_3 membranes prepared by (A) PPM, (B) CV, (C) PD, (D) GD, and the PXa layer prepared by PPM without Fe_2O_3 (E).

EIS is very sensitive to the changes in interfacial impedance of the electrodes upon biorecognition events occurring at the electrode/electrolyte interface. The Bode plots of different modified electrodes were recorded in 0.3 mol/L PBS (pH 7.0) and shown in Fig. 3B. Obvious difference in the interface electron-transfer resistances of the above four modified electrodes could be observed especially in the high-frequency regions. After modification with nanosized Fe_2O_3, the impedance of Fe_2O_3/CPE became lower (curve b) compared with that of bare CPE (curve a). A further decrease of the impedance was observed at the PXa/CPE (curve c). However, the lowest impedance was obtained at the PXa/Fe_2O_3/CPE (curve d), demonstrating the lowest electron-transfer resistance. These results were in accordance with that of the CV studies.

3.5. *Influence of Fe_2O_3 on the formation of the PXa/Fe_2O_3 nanorhombi*

The influence of nanosized Fe_2O_3 on the formation of the PXa/Fe_2O_3 nanocomposite membranes was investigated. Two kinds of composite membranes were respectively fabricated by using two kinds of Fe_2O_3 addition modes. One was that a certain amount of Fe_2O_3 was firstly coated on the surface of CPE and then the polymerization was performed in the Xa monomer solution, denoted as PXa/Fe_2O_3. The other was copolymerization of Xa monomer and Fe_2O_3, denoted as PXa–Fe_2O_3. The self-redox signals of PXa at the two different types of composite membranes modified electrodes showed that the current response recorded at the PXa/Fe_2O_3/CPE was almost three times as large as that at

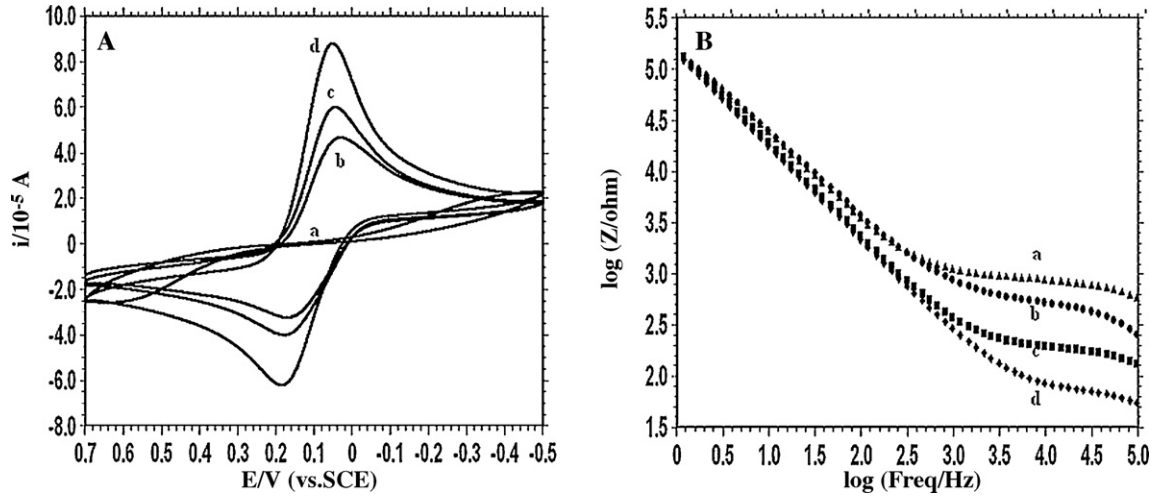

Fig. 3. (A) CVs of 1.0 mmol/L $[Fe(CN)_6]^{3-/4-}$ containing 0.1 mol/L KCl recorded at bare CPE (a), Fe_2O_3/CPE (b), PXa/CPE (c), and PXa/Fe_2O_3/CPE (d). Scan rate: 100 mV/s. (B) Bode plots of the electrodes corresponding to (A) recorded in 0.3 mol/L PBS (pH 7.0) under open-circuit conditions.

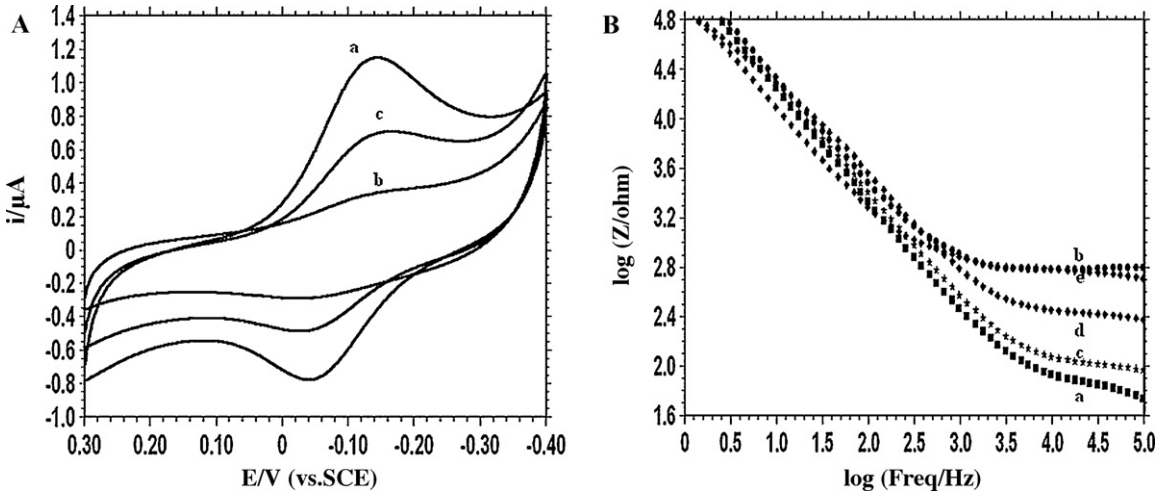

Fig. 4. (A) CVs of the PXa/Fe_2O_3 membranes before (a) and after probe ssDNA immobilization (b), hybridization reaction with cDNA (c) recorded in 0.3 mol/L PBS (pH 7.0). Scan rate: 100 mV/s. (B) Bode plots recorded at PXa/Fe_2O_3/CPE (a), ssDNA/PXa/Fe_2O_3/CPE (b), dsDNA/PXa/Fe_2O_3/CPE (hybridized with cDNA (c)), the probe electrode hybridized with single-base mismatched DNA (d), the probe electrode hybridized with ncDNA (e) in 0.3 mol/L PBS (pH 7.0) under open-circuit conditions.

the PXa–Fe_2O_3/CPE. Therefore, the existence form of nanosized Fe_2O_3 in the electropolymerization process had an obvious effect on the electrochemical performance of the formed nanocomposite membranes. The coated Fe_2O_3 could form a uniform and compact membrane on the CPE and act as the seeds, which could provide more growth sites for the formation of PXa.

The amount of Fe_2O_3 also had a pronounced effect on the performance of the composite membranes modified electrode. EIS was adopted to investigate the effect of the amount of Fe_2O_3 on the formation of the nanocomposite membranes. With the increase of the amount of Fe_2O_3, the impedance value of the PXa/Fe_2O_3 membranes reduced gradually, and the minimum was obtained at 10 μL of 2.0 mg/mL Fe_2O_3. When the amount of Fe_2O_3 was larger than 10 μL of 2.0 mg/mL, the impedance value increased. This might be due to the coverage of the electrode surface by an extremely thick membrane of Fe_2O_3, which might prevent the effective adsorption and polymerization of PXa, resulting in the depressed conductivity of the formed composite membranes. Thereby, 10 μL of 2.0 mg/mL Fe_2O_3 was selected for the electrode modification in our experiments.

3.6. CV and indicator-free impedance monitoring of DNA immobilization and hybridization

The self-redox properties of the PXa layer were investigated to monitor the immobilization and hybridization of DNA on the PXa/Fe_2O_3 membranes by the CV and EIS techniques in PBS (pH 7.0). As shown in Fig. 4A, curve a, a couple of well-shaped redox peaks were observed. This might be ascribed to the self-redox reactions of PXa that occur at the electrode surface. When the ssDNA probes were covalently immobilized on the PXa/Fe_2O_3 membranes through the EDC/NHS cross-linking reaction, the self-redox peaks of PXa decreased significantly, as shown in curve b. This could be due to the flexible traits and negatively charged phosphate backbones of the ssDNA probes. After immobilization, the ssDNA probes changed the conformation and blocked the effective electron transfer along the PXa chains. The obvious decrease of the CV signals compared with those of the PXa/Fe_2O_3 membranes was a powerful proof that the ssDNA probes had been successfully immobilized on the PXa/Fe_2O_3 membranes. After the ssDNA probes immobilized on the PXa/Fe_2O_3 membranes were hybridized with the cDNA,

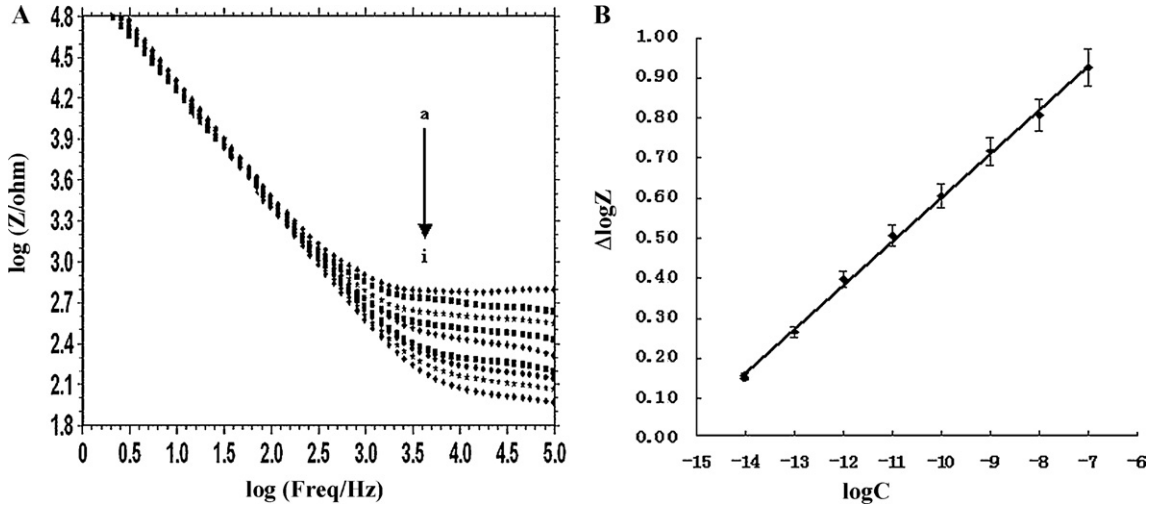

Fig. 5. (A) Bode plots recorded at the ssDNA/PXa/Fe_2O_3/CPE (a) and after hybridization reaction with different concentrations of PML/RARA fusion gene target sequences: (b) 1.0×10^{-14} mol/L, (c) 1.0×10^{-13} mol/L, (d) 1.0×10^{-12} mol/L, (e) 1.0×10^{-11} mol/L, (f) 1.0×10^{-10} mol/L, (g) 1.0×10^{-9} mol/L, (h) 1.0×10^{-8} mol/L and (i) 1.0×10^{-7} mol/L. (B) The plot of $\Delta \log Z$ vs. the logarithm of PML/RARA fusion gene target sequence concentrations. Conditions were the same as in Fig. 4B.

an increase of the CV signals in comparison with those originated from the CV of the probe-captured electrode was observed (curve c). Interpretation of the current enhancement upon hybridization might be proposed on the basis of changes in the conformation of DNA. Indeed, the ssDNAs behave as random coils while the dsDNAs (resulting of hybridization with the complementary target DNA) lead to a more organized surface, through which counter ions along the double-helix structure could diffuse more freely (Pham et al., 2003). At the same time, with the 18-mer ssDNA used in this study ssDNA is a flexible molecule while dsDNA acts as a rigid rod, and hence the electron transfer rate along the double-helix structure is much faster than that along the single-chain structure (Gooding et al., 2003). Therefore, the self-redox CV signals of polymerization membranes increased after the hybridization of ssDNA with its cDNA. The results indicated that the self-redox signals of the PXa layer could be used to directly detect target DNA by CV without an additional labeling step for the DNA target with signaling molecules.

The DNA immobilization and hybridization were also confirmed by EIS without the use of electroactive indicator such as $[Fe(CN)_6]^{3-/4-}$. The EIS measurements were carried out in PBS (pH 7.0) in the frequency range from 10^5 Hz to 1 Hz, and the Bode plots were shown in Fig. 4B. Curve a was the Bode plot of the PXa/Fe_2O_3/CPE. When the ssDNA probes were covalently immobilized on the PXa/Fe_2O_3 nanorhombi, the impedance increased obviously (curve b), especially in the high-frequency regions, indicating that the probe ssDNA had been successfully immobilized on the membranes. After hybridization with the cDNA (curve c), an evident decrease of the impedance was observed. There are mainly two factors that may influence the change of impedance of the electrode after DNA hybridization. On one hand, it is well-known that dsDNA is more conductive than ssDNA (Lee and Shim, 2001; Gu et al., 2005; Fu et al., 2005). On the other hand, the DNA molecules can modulate the work function and the double layer thickness at the surface of the electrode due to the intrinsic negative charge of DNA molecules (Thompson et al., 2005; Yan et al., 2009; Lin et al., 2011). In this experiment, when the hybridization reaction occurs, an obvious decrease of impedance values was observed, indicating that the first factor may occupy the chief status. And therefore the decrease of impedance after DNA hybridization in this experiment can be attributed to the much higher conductivity properties of dsDNA compared to ssDNA. Obviously, the PXa/Fe_2O_3 membranes could be employed for indicator-free direct electrochemical detection of DNA hybridization by EIS. The indicator-free impedance DNA biosensor was also used to distinguish different DNA sequences including single-base mismatched and ncDNA sequences. As shown in Fig. 4B, when the ssDNA/PXa/Fe_2O_3/CPE was hybridized with the single-base mismatched sequences, the impedance decreased (curve d). However, the decrease of the impedance value was much smaller than that obtained from the hybridization with the cDNA (curve c), which indicated that the complete hybridization was not accomplished due to the base mismatch. In addition, as expected, no significant difference of the impedance values could be observed for the ssDNA/PXa/Fe_2O_3/CPE (curve b) and its hybridization with the ncDNA sequences (curve e), since no successful hybridization occurred due to the sequence mismatch between the probe ssDNA and the ncDNA. These results demonstrated that the indicator-free impedance biosensing assay based on the PXa/Fe_2O_3 membranes had good selectivity.

3.7. Quantitative analysis of PML/RARA fusion gene target sequences

The probe-captured PXa/Fe_2O_3 membranes were used to quantitatively detect the PML/RARA fusion gene target sequences, and the Bode plots were obtained after hybridization with different concentrations of the complementary target sequences (Fig. 5A). The difference (namely $\Delta \log Z$) between the $\log Z$ values of the probe-captured electrode and that after hybridization with the cDNA was adopted as the measurement signal. The $\Delta \log Z$ value was linear with the logarithm of the PML/RARA fusion gene target sequence concentrations in the range from 1.0×10^{-14} mol/L to 1.0×10^{-7} mol/L with a correlation coefficient (R) of 0.9972 (Fig. 5B). The regression equation was $\Delta \log Z = 0.1102 \log C + 1.7025$, and a detection limit of 2.8 fmol/L could be calculated using 3σ (where σ was the relative standard deviation of the blank solution, $n = 11$). Thus the suggested indicator-free impedance detection assay was very efficient for ultrasensitive direct electrochemical detection of DNA hybridization.

3.8. Stability, reusability and reproducibility of the DNA biosensor

See Supplementary material for details.

4. Conclusions

An innovative electrochemical DNA sensing system for the covalent binding of capture probe onto the PXa/Fe_2O_3 nanorhombus membranes was for the first time developed. By combining with an indicator-free impedance technique, the developed protocol yielded an extremely high sensitivity, a wide linear range of 8 orders of magnitude, a femtomolar level detection limit and a fine selectivity for the hybridization event without a labeling step for the DNA target. It is thus expected that such an architecture of ssDNA immobilization combined with indicator-free EIS transduction will be useful for the development of DNA sensing devices.

Acknowledgments

This work was supported by the National Natural Science Foundation of China (No. 20805025, 20975057) and the Foundation of Qingdao City (No. 09-1-3-25-jch).

Appendix A. Supplementary data

Supplementary data associated with this article can be found, in the online version, at doi:10.1016/j.bios.2011.10.015.

References

Adekunle, A.S., Agboola, B.O., Pillay, J., Ozoemena, K.I., 2010. Sens. Actuators B 148, 93–102.
Bo, Y., Yang, H.Y., Hu, Y., Yao, T.M., Huang, S.S., 2011. Electrochim. Acta 56, 2676–2681.
Cao, S.W., Zhu, Y.J., 2008. J. Phys. Chem. C 112, 6253–6257.
Cash, K.J., Heeger, A.J., Plaxco, K.W., Xiao, Y., 2009. Anal. Chem. 81, 656–661.
Dong, H.F., Yan, F., Ji, H.X., Wong, D.K.Y., Ju, H.X., 2010. Adv. Funct. Mater. 20, 1173–1179.
Fu, Y.Z., Yuan, R., Xu, L., Chai, Y.Q., Zhong, X., Tang, D.P., 2005. Biochem. Eng. J. 23, 37–44.
Gooding, J.J., Chou, A., Mearns, F.J., Wong, E., Jericho, K.L., 2003. Chem. Commun., 1938–1939.
Gu, H.R., Su, X.D., Loh, K.P., 2005. J. Phys. Chem. B 109, 13611–13618.
Haccoun, J., Piro, B., Tran, L.D., Dang, L.A., Pham, M.C., 2004. Biosens. Bioelectron. 19, 1325–1329.
Hu, Y.W., Yang, T., Wang, X.X., Jiao, K., 2010. Chem. Eur. J. 16, 1992–1999.
Jiang, C., Yang, T., Jiao, K., Gao, H.W., 2008. Electrochim. Acta 53, 2917–2924.
Kannan, B., Williams, D.E., Booth, M.A., Travas-Sejdic, J., 2011. Anal. Chem. 83, 3415–3421.
Kjallman, T.H.M., Peng, H., Soeller, C., Travas-Sejdic, J., 2008. Anal. Chem. 80, 9460–9466.
Lee, T.Y., Shim, Y.B., 2001. Anal. Chem. 73, 5629–5632.
Lin, P., Luo, X.T., Hsing, I.M., Yan, F., 2011. Adv. Mater. 23, 4035–4040.
Liu, S.F., Liu, J., Han, X.P., Cui, Y.N., Wang, W., 2010. Biosens. Bioelectron. 25, 1640–1645.
Marques, P.R.B.O., Lermo, A., Campoy, S., Yamanaka, H., Barbe, J., Alegret, S., Pividori, M.I., 2009. Anal. Chem. 81, 1332–1339.
Peng, H., Zhang, L.J., Soeller, C., Travas-Sejdic, J., 2009. Biomaterials 30, 2132–2148.

Pham, M.C., Piro, B., Tran, L.D., 2003. Anal. Chem. 75, 6748–6752.
Prusty, D.K., Herrmann, A., 2010. J. Am. Chem. Soc. 132, 12197–12199.
Riccardi, C.S., Kranz, C., Kowalik, J., Yamanaka, H., Mizaikoff, B., Josowicz, M., 2008. Anal. Chem. 80, 237–245.
Sassolas, A., Leca-Bouvier, B.D., Blum, L.J., 2008. Chem. Rev. 108, 109–139.
Sharon, E., Freeman, R., Willner, I., 2010. Anal. Chem. 82, 7073–7077.
Shen, L., Ji, H.F., 2008. Dyes Pigments 76, 646–649.
Shiddiky, M.J.A., Torriero, A.A.J., Zeng, Z.H., Spiccia, L., Bond, A.M., 2010. J. Am. Chem. Soc. 132, 10053–10063.
Silva, F.A.S., Lopes, C.B., Costa, E.O., Lima, P.R., Kubota, L.T., Goulart, M.O.F., 2010. Electrochem. Commun. 12, 450–454.
Singh, R., Verma, R., Kaushik, A., Sumana, G., Sood, S., Gupta, R.K., Malhotra, B.D., 2011. Biosens. Bioelectron. 26, 2967–2974.
Solanki, P.R., Kaushik, A., Chavhan, P.M., Maheshwari, S.N., Malhotra, B.D., 2009. Electrochem. Commun. 11, 2272–2277.
Thompson, L.A., Kowalik, J., Josowicz, M., Janata, J., 2003. J. Am. Chem. Soc. 125, 324–325.
Thompson, M., Cheran, L.E., Zhang, M.Q., Chacko, M., Huo, H., Sadeghi, S., 2005. Biosens. Bioelectron. 20, 1471–1481.
Wang, J., Li, S.P., Zhang, Y.Z., 2010. Electrochim. Acta 55, 4436–4440.
Wei, N., Chen, J.H., Zhang, J., Wang, K., Xu, X.W., Lin, J.H., Li, G.W., Lin, X.H., Chen, Y.Z., 2009. Talanta 78, 1227–1234.
Yan, F., Mok, S.M., Yu, J.J., Chan, H.L.W., Yang, M., 2009. Biosens. Bioelectron. 24, 1241–1245.
Zhang, L., Ni, Y.H., Wang, X.H., Zhao, G.C., 2010. Talanta 82, 196–201.
Zhang, W., Yang, T., Li, X., Wang, D.B., Jiao, K., 2009a. Biosens. Bioelectron. 25, 428–434.
Zhang, X.Z., Jiao, K., Liu, S.F., Hu, Y.W., 2009b. Anal. Chem. 81, 6006–6012.
Zhou, Y., Yu, B., Guiseppi-Elie, A., Sergeyev, V., Levon, K., 2009. Biosens. Bioelectron. 24, 3275–3280.